Langmuir
Article
pubs.acs.org/Langmuir

Submicrometer Surface Patterning Using Interfacial Colloidal Particle Self-Assembly

Matthew A. Ray,[†] Nathan Shewmon,[‡] Sarang Bhawalkar,[‡] Li Jia,[‡,*] Yuzhen Yang,[§] and Eric S. Daniels[§]

[†]*Department of Chemistry, Lehigh University, Bethlehem, Pennsylvania 18015,* [‡]*Department of Polymer Science, University of Akron, Akron, Ohio 44325, and* [§]*Department of Chemical Engineering and Emulsion Polymer Institute, Lehigh University, Bethlehem, Pennsylvania 18015*

Received January 20, 2009. Revised Manuscript Received March 18, 2009

Hexagonal noncontiguously packed (HNCP) arrays of submicrometer-sized particles trapped at an air−water interface are successfully transferred to solid substrates. The long-range order of the hexagonal arrays at the interface can be improved by compression−relaxation cycles. The interparticle distance (i.e., the periodicity of the hexagonal array) can be controlled by varying the degree of compression of the particle film. The critical characteristics of the substrate surface are hydrophobicity (advancing water contact angle of $>70°$) and a charge complementary to the surface of the particles. Suitable silicon and glass substrates are easily prepared by treatment with commercially available organosilicon compounds. Two transfer processes have been developed. When the parallel transfer process is used, the HNCP arrays are deposited on the solid substrates with minimal pattern distortion. The vertical dipping transfer distorts the pattern and renders a sense of directionality perpendicular to the dipping direction. This surface patterning technique is applied to fabrication of subwavelength grating for antireflection in the visible region. Antireflective HNCP arrays comprising varied particle diameters and pattern periodicities are fabricated on glass substrates to demonstrate the effects of these parameters on the antireflection performance.

Introduction

Surface patterning using interfacially trapped particles can be traced back to an ancient oriental art developed more than 2000 years ago involving spreading pigment particles at an air−water interface to produce beautiful swirling patterns that were transferred to a piece of paper brought into contact with the surface of the water.[1] Modern scientific research in colloidal particles trapped at the air−water interface started in the 1960s[2,3] and has experienced a recent resurgence as a result of potential materials applications for the interfacial particle arrays including surface patterning at the submicrometer scale.[4−6] The surface patterning process usually first creates a hexagonal close-packed (HCP) monolayer of monodisperse spherical colloids at the air−water or alkane−water interface. The two-dimensional solid film is then transferred onto solid substrates for further hierarchical lithographic manipulations.

Distinct from the HCP arrays widely used for surface patterning is another type of two-dimensional hexagonal array, which was first reported by Pieranski in 1980.[7] The same charged particles in such hexagonal arrays at the air−water or alkane−water interface do not touch each other as the result of the exceptionally long-range interparticle electrostatic repulsions, which propagate through the nonpolar phase ($\varepsilon \approx 2$ for alkane and 1 for air, compared to ~80 for water).[8] The lattice constant can be several times the particle diameter and can be adjusted by varying the area of the confinement. To differentiate the two types of hexagonal lattices, we will refer to the latter type as a hexagonal noncontiguously packed (HNCP) lattice. The potential of such interfacial HNCP arrays for surface patterning is rather interesting because the HNCP surface features have practical applications. Other methods for patterning solid surfaces with the HNCP arrays have recently been developed.[9,10] The obvious challenge of using the interfacial HNCP arrays for such purpose is to preserve the order during a transfer process.[11] Prior to our study, attempts to transfer submonolayer particle films to solid substrates have always resulted in a loss of order, producing random particle films after transfer.[12,13] We have recently reported our success in transferring the HNCP arrays of micrometer-sized particles onto silicon wafers with the order intact.[14] In the work presented here, we describe the transfer of submicrometer-sized particles onto a variety of substrates and demonstrate the use of this method for the fabrication of the subwavelength moth-eye structures on glass for antireflection in the visible region.

*To whom correspondence should be addressed. E-mail: ljia@uakron.edu.

(1) Maurer-Mathison, D. *The Ultimate Marbling Handbook: A Guide to Basic and Advanced Techniques for Marbling Paper and Fabric*; Watson-Guptill: New York, 1999; pp 18.
(2) Schuller, H. *Kolloid-Z.* **1967**, *380*, 216–217.
(3) Sheppard, E.; Tcheurekdjian, N. *J. Colloid Interface Sci.* **1968**, *28*, 481–486.
(4) Binks, B. P. *Curr. Opin. Colloid Interface Sci.* **2002**, *7*, 21–41.
(5) Geissler, M.; Xia, Y. *Adv. Mater.* **2004**, *16*, 1249–1269.
(6) Wang, D.; Duan, H.; Moehwald, H. *Soft Matter* **2005**, *1*, 412–416.
(7) Pieranski, P. *Phys. Rev. Lett.* **1980**, *45*, 569–572.
(8) (a) Danov, K. D.; Kralchevsky, P. A.; Boneva, M. P. *Langmuir* **2006**, *22*, 2653–2667. (b) Horozov, T. S.; Aveyard, R.; Clint, J. H.; Binks, B. P. *Langmuir* **2003**, *19*, 2822–2829. (c) Aveyard, R.; Binks, B. P.; Clint, J. H.; Fletcher, P. D. I.; Horozov, T. S.; Neumann, B.; Paunov, V. N. *Phys. Rev. Lett.* **2002**, *88*, 246102-1-4. (d) Nikolaides, M. G.; Bausch, A. R.; Hsu, M. F.; Dinsmore, A. D.; Brenner, M. P.; Gay, C.; Weitz, D. A. *Nature* **2002**, *420*, 299–301. (e) Ghezzi, F.; Earnshaw J. C.; Finnis, M.; McCluney, M. *J. Colloid Interface Sci.* **2001**, *238*, 433–446. (f) Ruiz-Carcía, J.; Gámez-Corrales, R; Ivlev, B. I. *Phys. Rev. E* **1998**, *58*, 660–663. (g) Robinson, D. J.; Earnshaw, J. C. *Langmuir* **1993**, *9*, 1436–1438. (h) Armstrong, A. J.; Mockler, R. C.; O'Sullivan, W. J. *J. Phys.: Condens. Matter* **1989**, *1*, 1707–1730.
(9) (a) Min, W.-L.; Jiang, B.; Jiang, P. *Adv. Mater.* **2008**, *20*, 3914–3918. (b) Venkatesh, S.; Jiang, P.; Jiang, B. *Langmuir* **2007**, *23*, 8231–8235.
(10) Zhang, G.; Wang, D.; Gu, Z.-Z.; Hartmann, J.; Moehwald, H. *Chem. Mater.* **2005**, *17*, 5268–5274.
(11) Tieke, B.; Fulda, K. U.; Kampes, A. In *Nano-surface Chemistry*; Rosoff, M., Ed.; Marcel Dekker, Inc.: New York, 2002; pp 213−243.
(12) (a) Kumaki, J. *Macromolecules* **1986**, *19*, 2258–2263. (b) Kumaki, J. *Macromolecules* **1988**, *21*, 749–755.
(13) Fulda, K. U.; Tieke, B. *Supramol. Sci.* **1997**, *4*, 265–273.
(14) Ray, M. A.; Jia, L. *Adv. Mater.* **2007**, *19*, 2020–2022.

Experimental Section

Latex Particles. Monodisperse, positively charged poly(styrene-*co*-vinylimidazole) (PSV) latex particles of several sizes were synthesized by surfactant-free emulsion polymerization following a previously published procedure.[15] The latex particles were purified by serum exchange and ultracentrifugation and were stored as ~2.5 wt % dispersions. The dispersion was diluted with deionized water (Milli-Q, 15 MΩ) to 0.2 wt % before use. The particle sizes were measured by transmission electron microscopy on the basis of 300 individual particles for each sample, and the surface charge densities of the particles were measured by conductometric titration as summarized in Table 1.

Silicon Substrates. Sections of silicon wafers (25 mm × 25 mm) were placed vertically into a freshly prepared piranha solution (a 70:30 solution of concentrated sulfuric acid and 30% hydrogen peroxide) in a glass Coplin staining jar and kept under solution until use. **Caution:** *Piranha solution is a strong oxidizer that reacts violently with organic material and should be handled carefully*. Substrates were then removed, rinsed with at least 100 mL of deionized water dispensed from a squirt bottle, and dried with a nitrogen jet. Piranha-cleaned substrates had an advancing contact angle (θ_a) of 13 ± 2° (standard deviation, 19 measurements) and a receding contact angle (θ_r) that was too small to measure. The contact-angle measurements were performed using a Rame-Hart Inc. NRL CA goiniometer (model 100-00 115) using a Gilmont volumetric syringe to dispense buffered water at pH 7. The buffer was prepared by dissolving 3.40 g of KH_2PO_4 and 0.58 g of NaOH in 500 mL of deionized water. The average thickness of the native oxide layer remaining on the wafers after cleaning was determined by ellipsometry using a Rudolph Research Auto EL-III automatic ellipsometer with a HeNe Laser source at a wavelength of 632.8 nm and an angle of incidence of 70°. Using ellipsometer program 211 with a lower refractive index value of 1.46,[16] the native oxide layer thickness of the cleaned silicon wafer substrates was found to be 16.0 ± 0.4 Å (standard deviation, 33 measurements).[17]

Negatively charged hydrophobic self-assembled monolayers (SAMs) and noncharged hydrophobic SAMs were prepared by allowing clean silicon substrates to react with 2-(4-chlorosulfonylphenyl)ethyltrichlorosilane (SPTCS) and octadecyltrichlorosilane (OTS), respectively. Typically, 25 mL of anhydrous toluene and 10 drops of the SPTCS stock solution were placed into a glass Coplin staining jar under a nitrogen purge. The silicon substrates (prescored into fourths) were then placed vertically into the solution. The top of the jar was covered with parafilm, and a slight positive pressure of nitrogen was maintained in the jar. The substrates were allowed to react for 30 min, after which they were sequentially rinsed with toluene, THF, and deionized water and finally blown dry with a nitrogen jet. The substrates were then separated into 12.5 mm × 12.5 mm square sections and stored in a Petri dish until use. We measured the kinetics of SPTCS SAM formation by immersing a substrate into the reaction solution for 1 s, 1 min, 30 min, 1 h, and 20 h and measuring the contact angle and ellipsometric thickness (Figure 1). The curve reached a limiting value after reacting for several minutes. The final θ_a and θ_r of the OTS-modified silicon wafer were 96° and 72°, respectively.

Glass Substrates. Glass coverslips (2 cm × 2 cm) were first cleaned for at least 1 h in piranha solution at 60 °C. Cleaned slips were then rinsed with deionized water, dried with a nitrogen jet, and cut into fourths. Modification of the glass substrate with SPTCS alone gave a surface not sufficiently hydrophobic. Thus, the glass surface was modified with a mixture of (*p*-*tert*-butylphenyl)ethyltrichlorosilane (BPTCS) and SPTCS following the procedure described above for silicon wafers. The hydrophobicity of the glass substrate can be effectively varied by varying the ratio of SPTCS to BPTCS (Figure 2). The desired glass substrates with a θ_a of ~72° were obtained by adopting a 1:8 weight ratio of SPTCS to BPTCS. The optical transmittance of the glass substrate was measured on a Hewlett-Packard 8453 diode array spectrophotometer and compared with those of the glass substrates patterned by the HNCP particle arrays.

Table 1. Sizes and Polydispersities of PSV Particles Used in This Work

particle	D_N[a]	PDI[b]	σ[c] (μC/cm^2)	A[d] (Å^2/N$^+$)
PSV-258	258.0	1.003	20	80
PSV-208	208.6	1.005	18	73
PSV-136	136.6	1.013	17	67

[a] Number-average particle diameter. [b] PDI = D_W/D_N, where D_W is the weight-average particle diameter. [c] Charge density. [d] Parking area of the cationic imidazolium group.

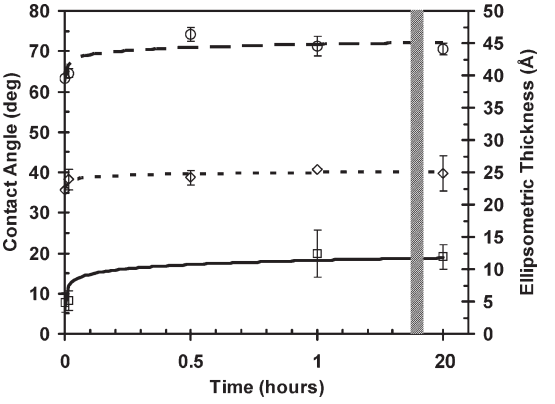

Figure 1. Kinetics of SAM formation on silicon substrate with SPTCS at 25 °C: (○) advancing contact angle with silicon substrate, (◇) receding contact angle with silicon substrate, and (□) ellipsometric thickness with silicon substrate. The lines were added as guides to the eye.

Stainless Steel Substrates. Mirror-finish stainless steel substrates from Pacific Plus International, Inc., were received with a protective PVC film covering the mirrored surface. Immediately after removal of the protective PVC film from the mirrored surface, the substrates could be used for particle transfer. The surface of the stainless steel substrates after removal of the protective PVC film was very hydrophobic, displaying a θ_a of 101 ± 3° (standard deviation, 10 measurements) and a θ_r of 38 ± 6° (five measurements). When the mirrored surface was buffed gently with 000 steel wool, rinsed with water, and dried with a nitrogen jet, the θ_a dropped to 35 ± 3° (11 measurements) and the θ_r to 10 ± 4°. XPS was performed on the mirrored surface immediately after the protective PVC film was removed. Strong carbon and oxygen peaks were observed, which could be greatly weakened by scratching the substrate while it was in the spectrometer and reanalyzing. No chlorine peaks were observed, which likely suggests that the protective PVC film was isolated from the steel surface by an adhesive layer. These data are consistent with our inference that a thin polymer film existed at the surface of the stainless steel substrates. Inquiries of the steel manufacturer concerning the presence of polymer film were made, but no reply was received. Nevertheless, the data strongly suggest that the mirrored steel was covered by a thin organic film.

Interfacial Particle Film Formation. Particle density at the air−water interface can be enriched by vortexing the latex dispersion. Typically, 10 mL of 0.2 wt % latex was placed into a 20 mL

(15) Kim, H.; Daniels, E. S.; Dimonie, V. L.; Klein, A. *J. Appl. Polym. Sci.* **2006**, *102*, 5753–5762.
(16) Rouse, J. H.; Ferguson, G. S. *J. Am. Chem. Soc.* **2003**, *125*, 15529–15536.
(17) When the surface oxide layer is thicker, for example, a thermally grown oxide layer, the method for glass surface modification should be used to achieve the necessary surface hydrophobicity.

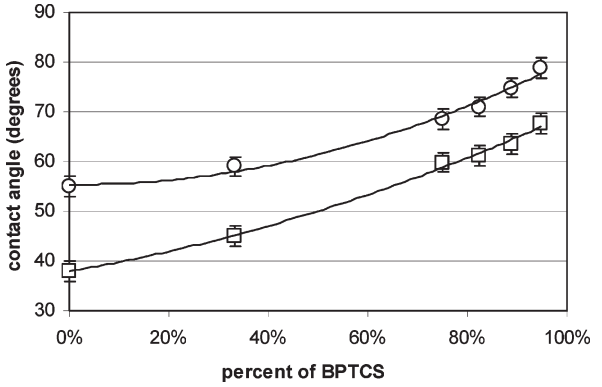

Figure 2. Change in the hydrophobicity of the glass surface modified with a mixture of SPTCS and BPTCS with various amounts of BPTCS in the mixture: (○) advancing contact angle with silicon substrate and (□) receding contact angle. The lines were added as guides to the eye.

scintillation vial. The area of the latex−air interface was increased as the liquid was vortexed. A significant number of latex particles became entrapped at the newly formed interface. Once vortexing was stopped, the surface area returned to the cross-sectional area of the vial. Highly compressed particle films were formed by this simple method. Alternatively, interfacial films with similar particle density can be generated by gently bubbling a nitrogen stream through the dispersion for 5 min. Both methods are used in the study.

Surface Pressure Isotherm. The above latex dispersion with a high surface particle density is used to fill a small Langmuir trough equipped with a Wilhemy balance and two mechanically driven barriers. The initial film area was 60 cm^2. The surface area−pressure isotherm is measured at a compression rate of 11.8%/min at room temperature. The order of the latex particle arrays can be drastically improved by compression−re-expansion cycles before the particles reach the densely packed state revealed by a sharp surface pressure upturn.

Transfer Processes. Two transfer methods were used in the study. In the first method (vertical transfer), the substrate was held perpendicularly with a forceps and was dipped through the interface after the particle film had achieved a desired state. This dipping process could be done by hand in a relatively quick vertical stroke. Alternatively, a homemade mechanical dipper was used to control the dipping rate.[18] The substrate was then directly withdrawn from the dispersion, rinsed with DI water, and blown dry with a nitrogen jet.

In the second method (parallel transfer), the appropriate substrate was fixed to the end of a dipping rod using double-sided tape. The substrate was slowly lowered manually in a parallel geometry into contact with the surface film after the particle film at the interface. After contacting the interfacial film, the substrate was lifted away from the interface. Excess water clinging to the substrate was either flicked off or rinsed off with deionized water. The substrate was then dried with a nitrogen jet.

Microscopy and Methods of Pattern Analysis. Scanning electron microscopy (SEM) was performed using a JEOL 6300f or JEOL JSM-7401F field emission scanning electron microscope. Scanning electron micrographs were processed using ImageJ[19] version 1.34s for pattern analysis and particle counting. SEM micrographs were analyzed by Fast Fourier transform (FFT) using ImageJ or Scion Image to extract particle spacing data, as well as information about the orientation and directionality of the images.

(18) Ray, M. A. Ph.D. Dissertation, Lehigh University, Bethlehem, PA, 2006.
(19) ImageJ analysis software is available free of charge at http://rsb.info.nih.gov/ij/.

Results and Discussion

Native Particle Films at the Air−Water Interface. Interfacial colloidal particle films are usually prepared by dispersing the colloids in an organic liquid and then spreading the dispersion at the air−water interface. The method cannot be applied to the particles used in this study. Even if only a few percent of alcohol was added to the aqueous suspension, the PSV latex coagulated and precipitated after several hours. As an alternative, population of the PSV particles onto the air−water interface was accomplished by vortexing or bubbling nitrogen through the latex dispersion. These methods are rather effective for creating a high particle density at the interface and induce simultaneous crystallization of the two-dimensional film when the agitation is stopped. A sheen appearance of the air−water interface demonstrates the crystalline nature of the native particle film. The ordered particle arrays can be transferred to a stainless steel substrate.[20] The SEM images of the transferred two-dimensional particle arrays reveal crystalline domains without significant long-range order (Figure 3).

Particle Film Crystallization in a Langmuir Trough. A Langmuir trough was used to investigate the crystallization of the two-dimensional particle film and to improve the long-range order of the particle film. After the sample had been vortexed, approximately 50 mL of the 0.2 wt % PSV-258 latex was poured into the Langmuir trough. The initial film area was 60 cm^2 and was compressed at a rate of 11.8%/min. The surface pressure (Π) isotherm was recorded and plotted as a function of the trough surface area (A) and compression ratio (Figure 4). To obtain the information concerning the length scale of interparticle interaction from the isotherm, the total number of particles at the interface must be known. Although the number of particles at the interface cannot be controlled experimentally, this quantity can be calculated from the point of the solid-phase transition as indicated by the abrupt increase in surface pressure when the interparticle distance is equal to the particle diameter. By extrapolating the solid transition to the area axis, we calculate the number of particles at the surface from the HCP packing area. The surface pressure can then be plotted as a function of a theoretical interparticle distance (D_h) assuming a single hexagonal lattice at all points. The $\Pi-D_h$ isotherm reveals that the PSV-258 particles do not begin to significantly interact with each other until they move within 100 nm of each other. Note that the $\Pi-D_h$ isotherm can be reproduced in separate experiments, but the surface pressure isotherms plotted as a function of the trough surface area or compression ratio are only superimposable after a shift in compression ratio by as much as 15% because the method of vortexing or bubbling cannot quantitatively produce the same particle density in separate attempts in spite of the identical sample preparation.

The interfacial PSV-258 particle films formed at various compression ratios are transferred by the parallel transfer method onto the stainless steel substrates and imaged by SEM (Figure 5). Apparently, the particles do not form any ordered arrays in the first compression cycle until the interparticle distance is very close to the particle diameter (Figure 5A−E). In a separate set of experiments, the film was first compressed to a compression ratio of 80% just before the anticipated solid transition occurs and the barrier was completely reopened. The second compression cycle was then performed, and the films were transferred at various compression ratios (Figure 5A′−E′). Clearly, the relatively

(20) Stainless steel was the first substrate that we found to work. As a result, the early experiments, including the study of the surface compression effect and the development of parallel and vertical transfer methods, were conducted with the stainless steel substrate.

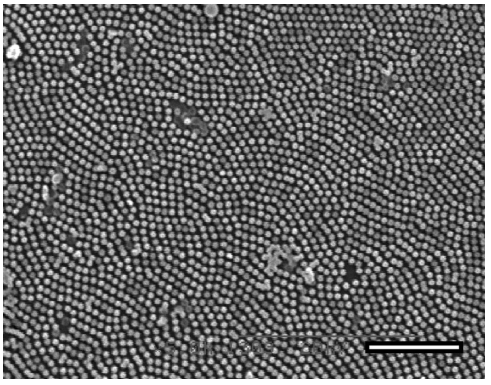

Figure 3. SEM micrographs of native PSV-258 particle arrays after they were transferred onto a stainless steel substrate. The scale bar is 5 μm.

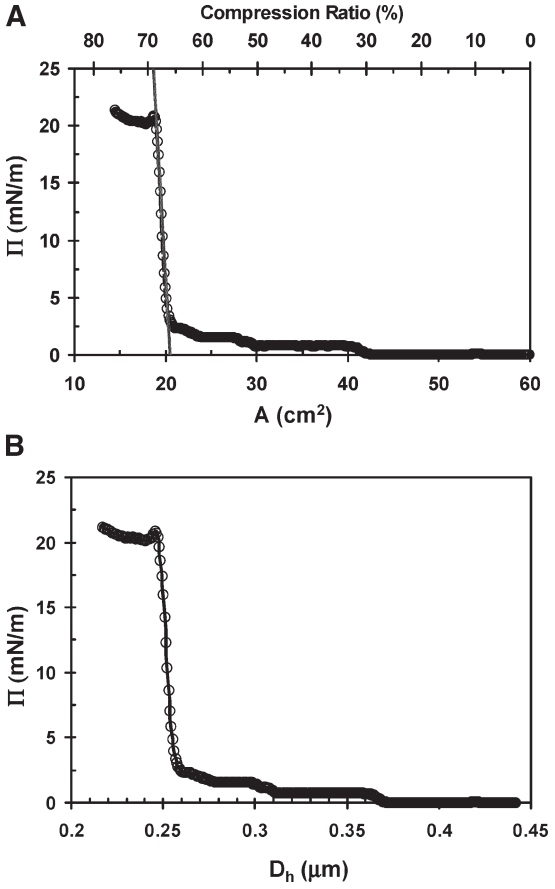

Figure 4. Surface pressure (Π) isotherms of 0.2 wt % PSV-258 latex. (A) Plotted as a function of both the trough area (A) and the surface film compression ratio. Extrapolation of the solid transition to the area axis produced the equation $y = -13.61x + 278.1$ ($R^2 = 0.9918$). The number of particles at the surface was found to be 3.544×10^{10}. (B) Plotted as a function of interparticle distance assuming hexagonal symmetry at all points (D_h).

long-range order of the film is retained during the compression−expansion cycle. Solid substrates decorated with HNCP arrays with controlled interparticle distances can be obtained this way. Caution must be taken to avoid compressing the interfacial film past the two-dimension solid transition, at which point the particles would become irreversibly jammed. Alternatively, to achieve the HNCP lattice, the compression−expansion cycles can be performed several times, but each compression stops at a compression ratio well before the two-dimensional solid phase is reached.

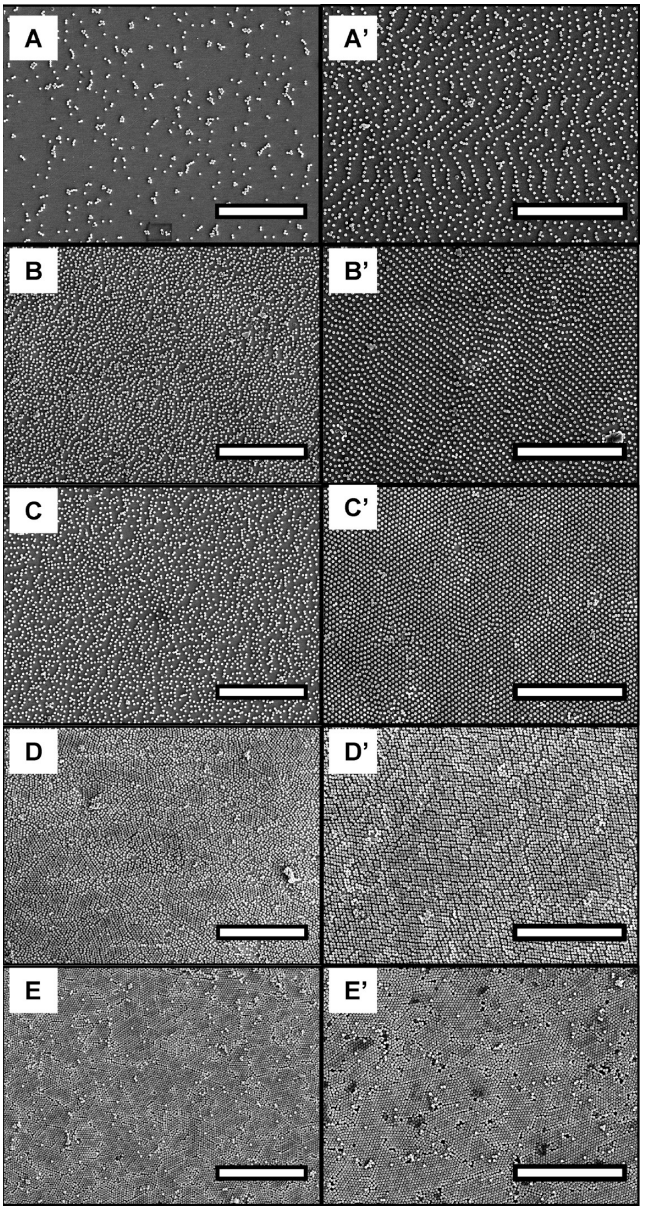

Figure 5. PSV-258 particle arrays transferred to mirror-finish stainless steel substrates by the parallel transfer method: (A−E) first compression cycle and (A′−E′) second compression cycle. Compression ratios were as follows: (A and A′) 0%, (B and B′) 20%, (C and C′) 40%, (D and D′) 60%, and (E and E′) 80%. The scale bars are 10 μm.

Pattern Distortion by Vertical Transfer. The patterns obtained by the vertical transfer process are distorted with the hexagons overall stretched in the dipping direction as unambiguously revealed by fast Fourier transform (FFT) analysis of the SEM image (Figure 6). The general sense of directionality is perpendicular to the dipping direction. Because the exact outcome of the distortion is apparently dependent on the original orientation of the HNCP crystalline grains with respect to the dipping direction, a variety of appearances were created due to the presence of multiple crystalline grains at the air−water interface. For this reason, it proved very difficult to study the distortion process in detail at least with the present particle systems.[18] Here, we tentatively suggest only two possible sources that may create the distortion. First, judging from the fact that the entire area dipped through the air−water interface is covered with the particle arrays, the air−water interface must be pinned on the

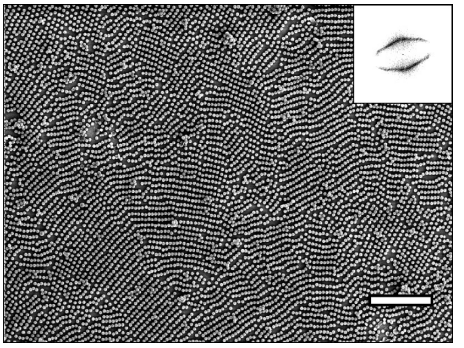

Figure 6. Distorted pattern by vertical transfer onto a stainless steel substrate. The scale bar is 5 μm. FFT of the image in the inset reveals the overall stretching direction of the unit cells of all crystal domains included in all the images.

back of the particles after the particles are adsorbed on the substrate.[21] Stick−slip motion subsequently may generate the sense of directionality of the pattern.[22] Second, a shear force caused by the vertical dipping may distort the particle arrays. Distortion of particle monolayers trapped at an air−water interface by shear forces has previously been reported.[23] Parenthetically, although pattern distortion was also occasionally observed in parallel transfer (Figure 5A′,B′), the occurrence and direction of the distortion were random. In these cases, the distortion is undoubtedly caused by stochastic factors, such as surface vibration or imperfect parallel geometry between the substrate and the interface at the point when the substrate is brought into contact with the interfacial film.

Role of Surface Charge in Pattern Transfer. We have confirmed that hydophobicity is a necessary attribute for successful pattern transfer (see more discussion below), but it remains unclear whether electrostatic attraction between the substrate and the particles is essential for preserving the pattern as we assumed at the onset of the research.[14] While the mirror-finish stainless steel substrate works very well for pattern transfer, its surface charge proves to be difficult to characterize because of the conducting nature of the bulk material. To probe this question as well as being motivated by the widespread applications of patterned silicon surfaces, we prepared the SPTCS- and OTS-modified silicon wafers as the patterning substrates. The OTS-functionalized silicon substrates most likely have a lower effective surface charge but are more hydrophobic (θ_a = 96°) than the silicon substrates bearing SAMs derived from SPTCS (θ_a = 72°). The ability of such SPTCS-functionalized silicon wafers is essentially identical to that of the stainless steel substrates (Figure 6 vs Figure 7A), but the OTS-functionalized silicon substrate appears to be less capable of preserving the pattern. The largest difference between the two substrates is observed in the vertical transfer process. Different patterns result on the substrates even if the transfer is performed at an identical dipping rate (11.8 mm/s) using a mechanical dipper (Figure 7). On the OTS-treated substrate, adjacent particle lines were squeezed together to form the bundled-up lines, indicating that the strength of the particle−octadecylsiloxane interaction is insufficient for overcoming the destructive lateral capillary forces during drying. In comparison, the bundled-up lines were absent on the SPTCS-functionalized

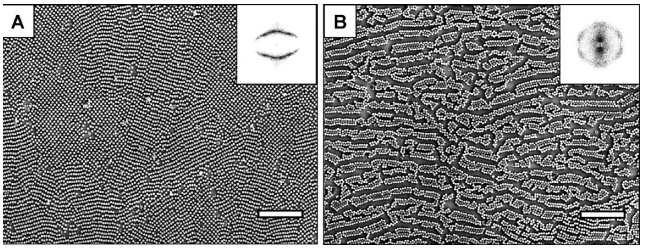

Figure 7. Surface charge dependence of vertical transfer. (A) Pattern on an SPTCS-functionalized silicon substrate. (B) Pattern on an OTS-functionalized silicon substrate. The substrates were dipped downward. The scale bars are 5 μm. The insets are the FFTs of the images.

substrate. The electrostatic attraction evidently does play a noticeable role in the pattern transfer process.

Fabrication of Moth-Eye Antireflection Structure on Glass. Subwavelength periodic structures discovered on the corneas of moth eyes[24] reduce Fresnel reflection by creating a gradient of refractive index effectively blurring the interface of reflection.[25,26] The moth-eye antireflective structure has potential technological advantages over the conventional thin-film antireflection coating for achieving broadband, wide incidence angle antireflection. As one of the possible applications of the surface patterning technique utilizing interfacial HNCP colloidal arrays described above, the moth-eye structure is fabricated on glass substrates as a proof of feasibility. We choose to use glass substrates because the difference in refractive index between the polystyrene latex particles and glass is small enough that no further pattern transfer technique such as dry etch is necessary for the initial demonstration.

The glass substrates are functionalized by a mixture of SPTCS and BPTCS in an ∼1:8 weight ratio to achieve a sufficiently hydrophobic surface [θ_a = 75 ± 3° (22 measurements)]. Particles with diameters of 136 and 208 nm (PSV-136 and PSV-208, respectively) were used so that subwavelength periodicity allowing antireflection in the entire visible region can be achieved. Again, after surface population by bubbling with nitrogen, the latex dispersions were poured into a small Nima Langmuir trough. The interfacial film was compressed in small steps with pauses between the steps, while the surface pressure was monitored with a Wilhelmy plate. Between two compression steps, the interfacial particle film was "annealed" as indicated by a slow decrease in surface pressure. It is assumed that during this "equilibration" period, the interparticle electrostatic repulsion drove the particles to self-assemble into the lowest-energy conformation, i.e., the HNCP arrays. As one would expect, higher surface pressure generally led to closer interparticle spacing. The parallel transfer was performed carefully so that only one side of the glass substrate contacted the particle film at the interface and carried the HNCP particle arrays. The substrate was then rinsed with deionized water and dried with a nitrogen jet.

Optical transmittance was measured to evaluate the antireflective function of the HNCP particle arrays. The representative samples with different particle diameters and HNCP lattice constants are compared (Figure 8). Both samples A and B are patterned with the PSV-136 particles, but the lattice constants of the HCNP arrays are 242 nm (±4 nm, standard deviation of 18 measurements) and 281 nm (±11 nm, standard deviation of 18 measurements), respectively. The HNCP arrays with the lattice

(21) de Gennes, P. G. *Rev. Mod. Phys.* **1985**, *57*, 827–863.
(22) Ray, M. A.; Kim, H.; Jia, L. *Langmuir* **2005**, *21*, 4786–4789.
(23) (a) Stancik, E. J.; Gavranovic, G. T.; Widenbrant, M. J. O.; Lasckitsch A. T.; Vermant, J.; Fuller, G. G. *Faraday Discuss.* **2003**, *123*, 145–156. (b) Stancik, E. J.; Hawkinson, A. L.; Vermant, J.; Fuller, G. G. *J. Rehol.* **2004**, *48*, 159–173.
(24) Bernhard, G. *Endeavour* **1967**, *26*, 79.
(25) Clapham, P. B.; Hutley, M. C. *Nature* **1973**, *244*, 281–282.
(26) Southwell, W. H. *J. Opt. Soc. Am. A* **1991**, *8*, 549–553.

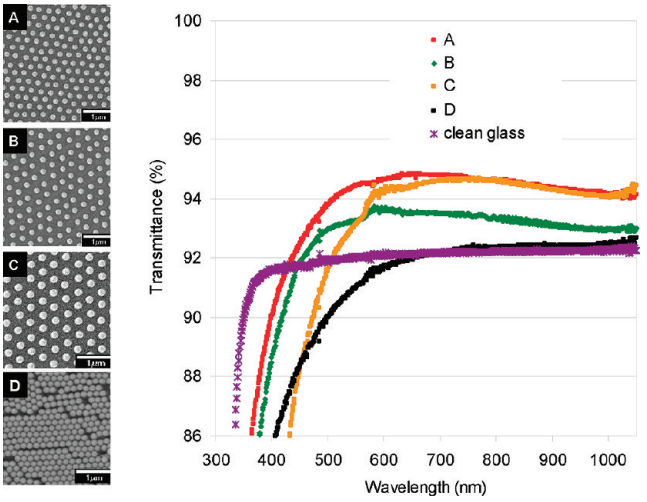

Figure 8. SEM images (left) and optical transmittance (right) of glass slides coated with hexagonal particle arrays: (A) PSV-136 particles with a lattice constant of 242 nm, (B) PSV-136 particles with a lattice constant of 281 nm, (C) PSV-208 particles with a lattice constant of 362 nm, and (D) PSV-136 particles with a HCP array. The HNCP lattice constants were obtained by FFT of the SEM images. The alphabetic labels correlate the SEM images to the transmittance curves.

constant of 242 nm (sample A) start to exert an antireflective effect compared to the unfunctionalized clean glass at a wavelength of ~425 nm. In comparison, the HNCP arrays with a lattice constant of 281 nm (sample B) begin to improve the transmittance at a wavelength of ~445 nm. After the respective critical wavelengths, the denser HNCP arrays on sample A also exert a better antireflection effect than the looser HNCP arrays on sample B likely because the denser particle arrays generate a more gradual change in the refractive index. Both the particle size and the lattice constant of sample C are greater than those of samples A and B. The large periodicity of the pattern pushes the critical wavelength of antireflection to ~500 nm. These observations are consistent with the theoretical notion that the minimum functional wavelength of an antireflective subwavelength grating is determined by the periodicity of the grating.[27] In the red to near-infrared region (wavelengths of > 700 nm), the transmittances of samples A and C are rather comparable and are both better than that of sample B. The larger PSV-208 particles in sample C likely create a more favorable gradient of refractive index in the vertical direction than the PSV-136 particles in sample B despite the larger lateral periodicity in sample C and therefore render a better antireflection effect after the critical wavelengths.[28] Finally, the dense HCP particle arrays (sample D) do not generate enough gradient of refractive index to significantly reduce reflection.

Requirements for Particle Transfer and Pattern Preservation. Transfer of the interfacial HNCP particle arrays onto a solid substrate can be conceptualized as a two-part problem: (1) the complete transfer of all particles from the air−water interface onto a solid substrate and (2) preservation of the HNCP pattern against destructive capillary force during drying.[14] Hydrophobic attraction between the particles and the substrate is a necessary and likely sufficient element for the first part. Complete transfer of the interfacial particles is achieved for all aforementioned substrates with a water θ_a of ~70° or larger, including stainless steel, surface-modified silicon, and surface-modified glass. After they are transferred onto the solid substrate, the particles are subjected to a strong lateral capillary force during the drying process.[29] It appears to be more difficult to preserve the pattern after the particles are on the solid substrate than to transfer them onto the solid substrate. In particular, the patterns with small interparticle distances are increasingly difficult to preserve because the lateral capillary force on a pair of neighboring particles is inversely proportional to the interparticle distance,[29] as manifested by comparison of images C versus D and C′ versus D′ in Figure 5. Among the substrates explored in this work, the ability of preserving the pattern is identical for mirror-finish stainless steel substrate, SPTCS-modified silicon substrate, and BPTCS/SPTCS-modified glass substrate, but the OTS-modified silicon substrate appears to be inferior due to the absence of the attractive electrostatic interactions. Finally, it is worth noting that in our previous report using the micrometer-sized polystyrene particles with sulfonate surface-functional groups,[14] an additional fluid-exchange process is necessary to preserve the pattern from being destroyed by the capillary force. The additional step is not necessary for the PSV particles used in this work. Therefore, the inherent adhesion property of the particles is also important for the successful pattern transfer.

Conclusions

HNCP arrays of submicrometer-sized particles trapped at the air−water interface are successfully transferred onto solid substrates. The critical characteristics of the suitable substrate surfaces are hydrophobicity and a charge complementary to the surface of the particles. Suitable silicon and glass substrates are easily prepared with commercially available organosilicon compounds. Commercial mirror-finish stainless steel is also found to be an excellent substrate. Two transfer processes can be used. When the parallel transfer process is used, rapid adhesion and transfer was achieved with minimal disturbance of the HNCP pattern. The vertical dipping transfer distorts the pattern and renders a sense of directionality generally perpendicular to the dipping direction. This surface patterning technique is demonstrated to be applicable for fabrication of subwavelength surface grating for reduction of reflection in almost the entire visible region. A distinct feature of this method in forming the HNCP patterns is that the interparticle distance can be easily varied. An addition niche may prove to be patterning curved surfaces using these transfer techniques.

Acknowledgment. M.A.R. thanks the Department of Chemistry of Lehigh University for a research fellowship. Acknowledgment is also made to the National Science Foundation for support of N.S. through the University of Akron REU Site for Polymer Science and Engineering (DMR-0648318). L.J. thanks the Office of Research Services and Sponsored Programs of the University of Akron for a Faculty Research Grant.

(27) Grann, E. B.; Moharam, M. G.; Pommet, D. A. *J. Opt. Soc. Am. A* **1995**, *12*, 333–339.
(28) Raguin, D. H.; Morris, G. M. *Appl. Opt.* **1993**, *32*, 1154–1167.
(29) Kralchevsky, P. A.; Nagayama, K. *Langmuir* **1994**, *10*, 23–36.